



An Approach to the Development of LSCF/YSZ-SDCC Dual Composite Cathodes for Intermediate Temperature SOFCs

Nurul Farhana Abdul Rahman¹, Hamimah Abd Rahman^{1,*}, Umira Asyikin Yusop¹, Tan Kang Hui²

¹ Faculty of Mechanical and Manufacturing Engineering, Universiti Tun Hussein Onn Malaysia, 86400 Batu Pahat, Johor, Malaysia

² Department of Materials Engineering, Faculty of Engineering and Technology, Tunku Abdul Rahman University of Management and Technology, Jalan Genting Kelang, Setapak, 53300, Kuala Lumpur, Malaysia

ARTICLE INFO

Article history:

Received 27 April 2023

Received in revised form 1 July 2023

Accepted 11 July 2023

Available online 21 July 2023

Keywords:

Cathode; Dual Composite; ITSOFC; LSCF; Screen Printing; YSZ-SDCC

ABSTRACT

A development of dual composite cathode, $\text{La}_{0.6}\text{Sr}_{0.4}\text{Co}_{0.2}\text{Fe}_{0.8}\text{O}_{3-\delta}/\text{Y}_2\text{ZrO}_5\text{-Sm}_{0.2}\text{Ce}_{0.8}\text{O}_{1.9}$ carbonate (LSCF/YSZ-SDCC) has been studied subjected on the composition of YSZ-SDCC composite. LSCF/YSZ-SDCC dual composite powders were produced through the high-energy ball milling method with a varied composition of YSZ-SDCC composite powder (50-70 wt.% YSZ: 50- 30 wt.% SDCC). The calcined LSCF/YSZ-SDCC powders were then successfully screen-printed on YSZ pellet to form a cathode thin film. A complete symmetrical cell was sintered for 90 minutes at 600°C. The crystalline phase, the carbonate bonding and the physical morphologies of the YSZ-SDCC composite cathode powders and the LSCF/YSZ-SDCC dual composite cathode powders were investigated. Furthermore, the microstructure and cathode thin film properties including electrochemical performances of LSCF/YSZ-SDCC were all evaluated. The various processes did not affect the carbonate bonding in any of the samples, however, phase identification analysis revealed the appearance of strontium carbonate (SrCO_3) as the secondary phase in the calcined LSCF/YSZ-SDCC powders. The microstructure study of the particles after milling demonstrates that the particles for all three YSZ-SDCC compositions do not agglomerate, with grain sizes of 244.97 ± 40.66 , 213.47 ± 41.63 , and 173.27 ± 25.83 nm, respectively. Following that, all samples were electrochemically analyzed at temperatures of 700°C, 600°C, and 500°C. As compared to the other combinations, LSCF/YSZ-SDCC with 50:50 wt.% YSZ-SDCC compositions co-fired at 700°C showed the most favourable value in this study.

1. Introduction

A fuel cell is a device that uses a chemical reaction to turn hydrogen or gas into electricity [1]. As long as the energy source is available, fuel cells can continually create electricity; compare batteries which must be charged on a regular basis [1]. Proton exchange membrane fuel cells (PEMFC), direct methanol fuel cells (DMFC), phosphoric acid fuel cells (PAFC), molten carbonate fuel cells (MCFC), and solid oxide fuel cell (SOFC) are the most common types of fuel cells. SOFC is made up of two porous electrodes (cathode and anode) and separated by a dense of an electrolyte layer. An

* Corresponding author.

E-mail address: hamimah@uthm.edu.my

<https://doi.org/10.37934/aram.108.1.98110>

important aspect of solid oxide fuel cell (SOFC) technology is the choice of electrode material, which is determined by electrochemical performance, microstructure, and fabrication methods [2]. The cathode's performance must meet several critical criteria, including high mix-electronic-and-ionic conductivity to transport oxygen ions and electrons to the reaction sites. Additionally, the cathode's microstructure must provide numerous contact points for reactive gases, electronic conductors, and ionic conductors at the triple phase boundary to increase the number of electron transfer [2]. For the successful fabrication of a high performance SOFC, a cathode material must satisfy each of the following conditions: High ionic conductivity in an oxidizing environment within a range 0.001-0.1 S/cm, have greater resistance to cell performance loss brought on by chromium deposition, good thermal stability, and are catalysts for the oxygen reduction process [2]. Beyond that, cathodes must have a high electrical conductivity in the region of 100 S/cm as well as sufficient material porosity (20-40%) to aid in oxygen gas passage at the interface between the electrolyte and anode [3]. Moreover, the cathode material and electrolyte material need to be chemically compatible [4]. The choice of materials has benefited greatly by lowering the operating temperature of the cells. However, lowering the temperature below 800°C can result in inadequate catalytic activity of the selected material during the reduction process [5]. It is proposed to introduce a new type of material that can enhance the performance of the SOFC while decreasing its operating temperature. To overcome these obstacles, it will be necessary to thoroughly study potential ceramic materials, improve current fabrication methods, and use wide range of materials [6].

In this study, YSZ-SDCC composite powders were prepared with three different ratios. Y_2ZrO_5 (YSZ) is indeed a leading ceramic-based electrolyte for SOFC due to its excellent ionic conductivity, low cost, good bend strength, and high chemical inertness [7]. A lot of studies have used $Sr_{0.2}Ce_{0.8}O_{1.9}$ (SDC) because of its superior ionic conductivity, stability, and compatibility [5]. Interestingly, the ionic conductivity of doped ceria can be enhanced by using salts or hydrates like chlorides, fluorites, carbonates, and sulphates as a second phase. This is because these salts have been observed to conduct proton, which is compatible with the ion conductivity of oxygen [8]. The inclusion of carbonate in the composite cathode aids in enhancing the electrode's close proximity to the electrolyte interface, which can improve the ionic conductivity in the cell [9]. It once more increases the triple-phase boundary (TPB) to the full surface, enhanced the performance of the SOFC system. For that reason, this research concentrates on SDC carbonates rather than SDC material in the hopes that it will improve the performance of the cell. For the dual composite powder, YSZ-SDCC composite powders and $La_{0.6}Sr_{0.4}Co_{0.2}Fe_{0.8}O_{3-\delta}$ (LSCF) material were milled mechanically using a 50:50 wt. % ratio. At temperatures below 700°C, LSCF has outstanding ionic and electronic conductivity [10]. As a result, LSCF has gained popularity as an electrode material for SOFC applications at moderate temperatures.

2. Methodology

2.1 Powders Preparation

The SDCC electrolyte powder composed of 80 wt.% raw SDC powder (Kceracell, South Korea) and 20 wt.% binary carbonates, which are made up of 67 mol.% lithium carbonate (Li_2CO_3) and 33 mol.% sodium carbonates (Na_2CO_3) (Sigma Aldrich, USA), was prepared by low-speed ball milled for 24 hours followed by calcination process at 680°C [9]. From there on, the different weight ratios of YSZ powder (Kceracell, Korea) and aforementioned SDCC powder were ball milled (50:50, 60:40, and 70:30 wt. %) using high energy ball milling machine (HEBM) (Fritsch Pulveristte, Germany) for two hours at 550 rpm. Hence all the obtained YSZ-SDCC composite powders were subjected to calcination process at 680°C at a rate of 5°C/min for one hour.

The acquired YSZ-SDCC composite powders were mixed equally with a commercial LSCF powder (Kceracell, South Korea) to create LSCF/YSZ-SDCC dual composite cathode powders. Both powders were ball-milled in ethanol for 2 hours at 550 rpm, oven dried, and calcined at 750°C at a rate of 5°C/min in air for 1 hour. The prepared YSZ-SDCC composite cathode and LSCF/YSZ-SDCC dual composite cathode with a different composition are shown in Table 1.

Table 1

Prepared composite and dual composite powders samples

Composite Powders	Weight ratio composition (wt.%)	Denoted samples
YSZ-SDCC	50:50	YSC55
YSZ-SDCC	60:40	YSC64
YSZ-SDCC	70:30	YSC73
Dual Composite Powders		
LSCF/YSZ-SDCC	50/50:50	LYSC55
LSCF/YSZ-SDCC	50/60:40	LYSC64
LSCF/YSZ-SDCC	50/70:30	LYCS73

2.2 Preparation of Symmetrical Cells

YSZ electrolyte pellets (1mm thickness and 13mm diameter) were produced by the uniaxial pressing method using a manual hydraulic press (Bench Top 3851, Carver, USA). 1 ton weight pressure was applied with a holding time of 2 minutes for each pellet. On cathode components, the screen-printing technique was used to achieve consistent and considerable thickness [10]. LSCF/YSZ-SDCC dual composite cathode ink was screen printed on the top and bottom of the YSZ pellet to create a complete symmetrical cell. The LSCF/YSZ-SDCC dual composite ink was squeegeed through the 355 meshes onto the YSZ electrolyte pellet for 10 repetitions per layer (Figure 1). In details, formulation for dual composite cathode ink was created using the following ingredients: dual composite cathode powder, terpineol (solvent), oleic acid (dispersant), and ethyl cellulose (binding) [13]. All the ingredients were mixed manually using an agate mortar until the ink become slurry and achieved the desired viscosity. Subsequently, the obtained symmetrical cell was heat treated at 600°C in air atmosphere. A heat treatment above 600°C for the SDCC material has to be avoided in order to ensure that the value for the porosity of the SDCC is not less than 20% [14].

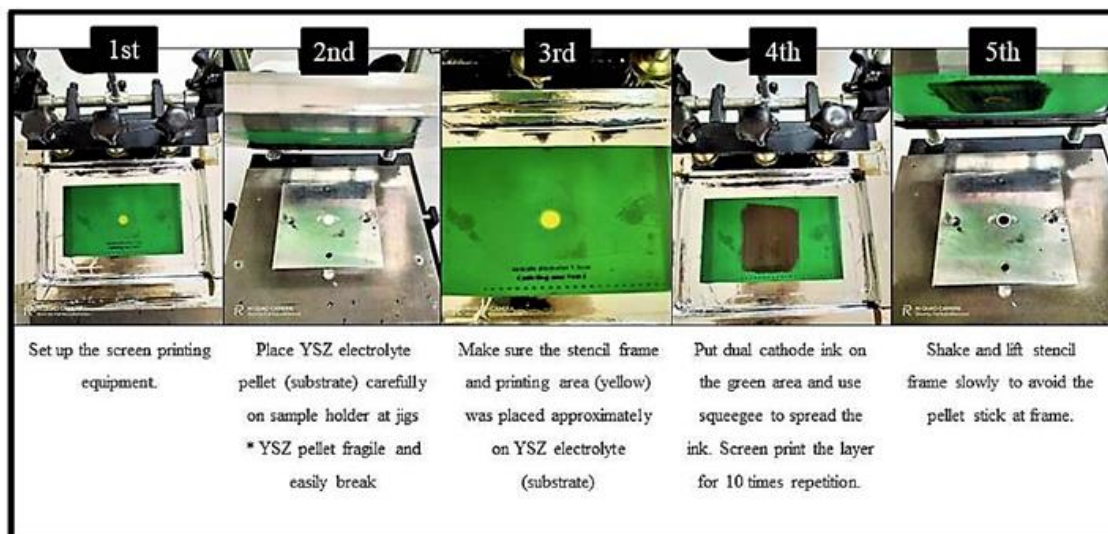


Fig. 1. Preparation of LSCF/YSZ-SDCC cathode thin film

2.3 Samples Characterization

X-ray diffraction (XRD; D8 Advanced Bruker, Germany) was used to determine the crystalline phases and the creation of any secondary phases in all the powders and cathode thin film that were created. To determine the presence of carbonates following various milling processes, Fourier transform infrared spectroscopy (FTIR; Perkin Elmer Spectrum 100, USA) was used. The infrared spectrum was captured in the wavelength range of 500 cm^{-1} to 4000 cm^{-1} . The microstructure of the produced powders was then investigated using field-emission scanning electron microscopy (FESEM; JSM 6380-Jeol, Japan). Using the micrographs acquired by FESEM, the particle sizes of all the generated powders were roughly approximated using the ImageJ software.

The electrochemical performance of the LSCF/YSZ-SDCC symmetric cell was measured over the temperature range 700°C and 600°C . The analysis of the polarization resistance and electrical conductivity in term of area specific resistance (ASR) of the dual composite cathode was measured using electrochemical impedance spectroscopy (EIS; Autolab 302, Eco Chemic, Netherlands) with a computer interface using NOVA software. The symmetrical cell was sandwiched between the platinum (Pt) mesh and the quartz (Figure 2). Pt meshes needs to be placed on the coating's surface for the current collector. The symmetrical cell configuration was then heated in the tube furnace (Berkeley, USA) to the desired temperature. The acquired impedance graph was being fitted and evaluated using the NOVA 1.10 software.

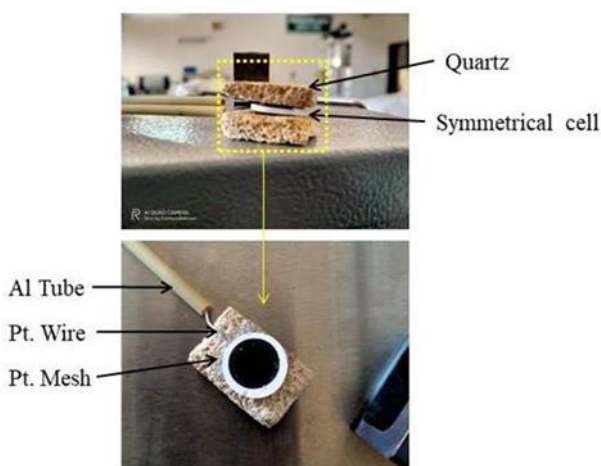


Fig. 2. Set up of the symmetrical cell

3. Results and Discussion

3.1 The Characteristics of the Prepared Powders

The XRD pattern for commercial powders of Li_2CO_3 , Na_2CO_3 , SDC, and milling SDCC composite powder is shown in Figure 3. The JCPDS numbers for Li_2CO_3 and Na_2CO_3 were 00-022-1141 and 01-070-9248, respectively. The JCPDS pattern number for SDC is 01-075-0157, and the SDCC diffraction may be validated using the same JCPDS pattern number as SDC, with a face-centered cubic lattice unit cell and space group of Fm3m. The SDCC composite did not demonstrate lithium carbonate or sodium carbonate diffraction peaks since the substances were present as amorphous phases that coated the powders during the calcination process. The resultant of the amorphous phase in the binary carbonates occurs at calcination temperatures of 680°C since this temperature is higher than their melting point of 600°C . It has been found that the amorphous state of the carbonate layer improves the ionic conduction for low-temperature solid oxide cells (LTSOFC) [11].

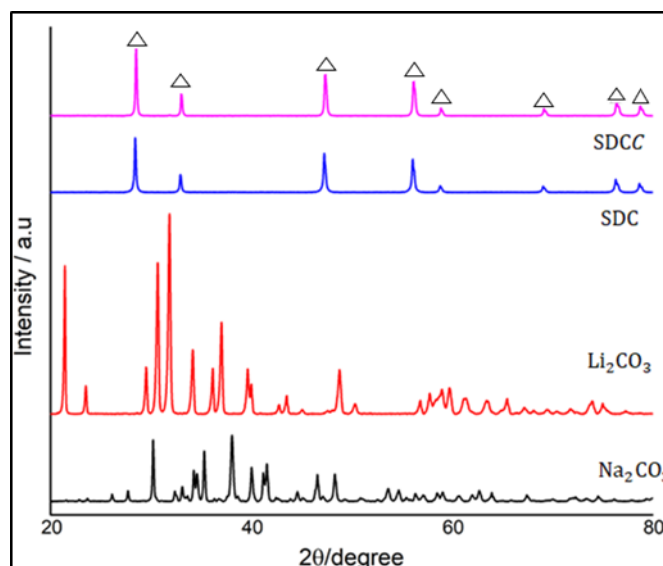


Fig. 3. XRD pattern for SDCC composite

The XRD diffraction patterns of YSZ-SDCC composite powders (YSC55, YSC64 and YSC73) are shown in Figure 4(a). No secondary phase was present, indicating good chemical compatibility between commercial YSZ and SDCC powders. The diffractograms were in correct alignment when the prepared YSZ-SDCC composite powders showed the same crystallite peak as YSZ and SDC raw material. Again, this demonstrates that only SDC has a well-defined fluorite crystal structure, whereas carbonates have an amorphous structure as aforementioned. YSZ has the JCPDS pattern number 00-030-1468 with a face centred cubic (FCC) lattice structure and the $Fm\bar{3}m$ space group. The generated YSZ-SDCC composite cathodes powders from three ratios demonstrated the appropriate intensity for each YSZ content and SDCC content, as shown in enlarged XRD pattern in Figures 4(b). The intensity of YSZ peaks grows as the composition ratio increases, whereas SDCC intensity decreases as the composition ratio decreases. This outcome can be viewed as proof that the rising ratio and rising YSZ electrolyte solid content are related.

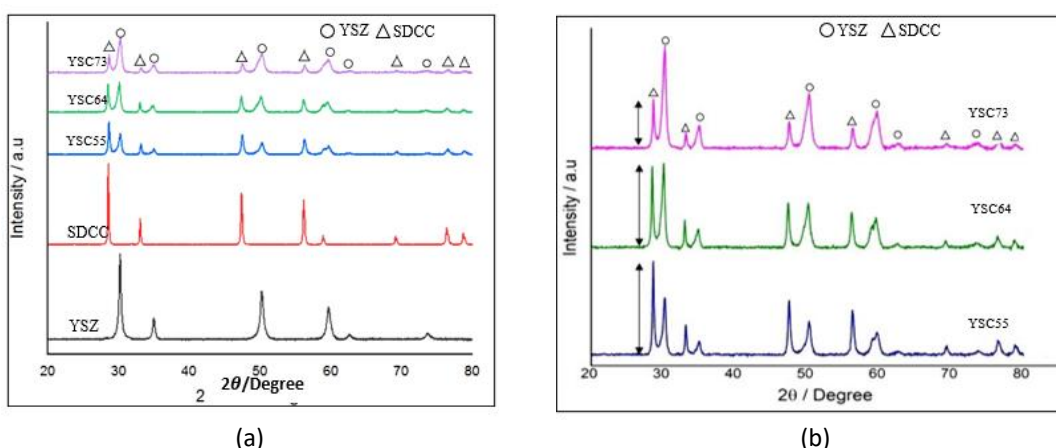


Fig. 4. (a) XRD pattern for YSZ-SDCC composite powders, (b) Enlargement XRD pattern

Afterwards, the YSZ-SDCC composite powders were combined with the LSCF powder to create LSCF/YSZ-SDCC dual composite powders. Figure 5(a) shows the XRD pattern of LSCF/YSZ-SDCC dual composite powder alongside with LSCF, YSZ, and SDCC powders. Secondary peaks were found in all three compositions of LSCF/YSZ-SDCC dual composite powders. Strontium carbonate (SrCO_3) with

JCPDS pattern number 00-005-0418 was observed. SrCO₃ exists as a secondary phase and has an orthorhombic lattice structure with the Pmcn (62) space group. The formation of a strontium carbonate peak might cause by the presence of strontium (Sr) element in La_{0.6}Sr_{0.4}Co_{0.2}Fe_{0.8}O_{3-δ} (LSCF) and carbonate, CO₃ in (Li/Na)₂CO₃ [15,16]. The existence of SrCO₃ after mixing with commercial LSCF powder might be attributed to the uncontrollable power created during the HEBM process, which triggered the formation of SrCO₃ [17]. There is a possibility that the presence of SrCO₃ as a secondary phase may degrade the performance of electrochemical cells. In order to determine the purity of the LSCF/YSZ-SDCC powder, the percentage of LSCF perovskite phase was determined using Eq. (1) provided by Swarts and Shrout [18]. For LYSC55, LYSC64, and LYSC73, the calculated perovskite phase percentages were 80.06%, 85.32%, and 81.19%, respectively. For lab-scale powder production, synthesized powders should have purity better than 90%. Obtaining absolute purity (100%) in lab-scale powder manufacturing is difficult [19].

$$\text{Perovskite phase} = \frac{I_p}{I_p + I_m} \times 100\% \quad (1)$$

where,

I_p = Maximum intensity of the perovskite phase

I_m = Maximum intensity of the impurity phase

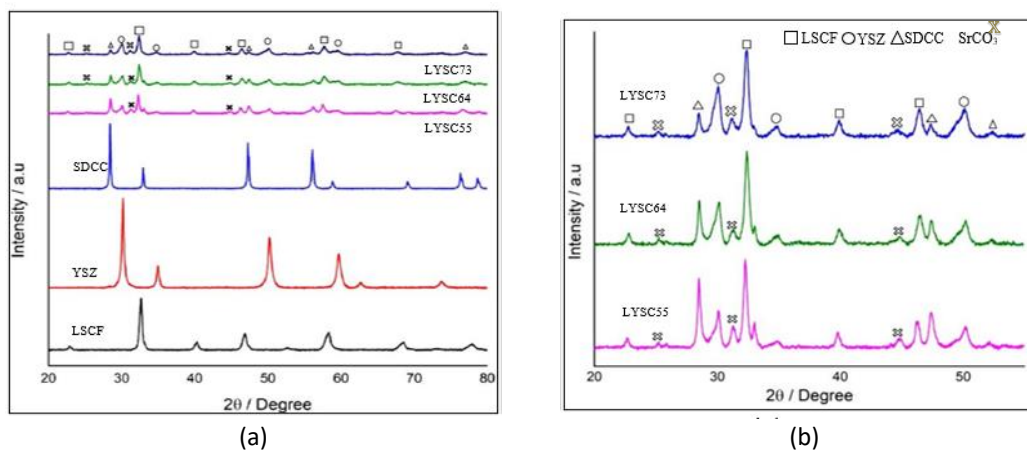


Fig. 5. (a) XRD pattern for LSCF/YSZ-SDCC composite powders, (b) Enlargement XRD pattern for LSCF/YSZ-SDCC dual composite powder

A FTIR analysis is employed to further clarify the existence of the carbonate layer on composite powders. Figure 6(a) shows the FTIR spectra of Li₂CO₃ and Na₂CO₃, SDC and SDCC powders. The binary carbonates exhibit transmission signals at 1410 cm⁻¹ and 1419 cm⁻¹ (stretching vibration) as well as 860 cm⁻¹ and 868 cm⁻¹ (bending vibration) where these peaks are associated with the absorption of carbonate ions (CO₃²⁻) [20]. An intense and broad peak was also found in the SDCC composite powder region at 1430 cm⁻¹ and 1506 cm⁻¹, as well as a sharp peak at 860 cm⁻¹, which corresponded to the vibration of the carbonate's ion. Figure 6(b) depicts FTIR spectra for commercial YSZ and SDC powders, manufactured SDCC, and three compositions of YSZ-SDCC composite powders. As expected, Due to the lack of any related constituents, the stretching and bending vibrations of the carbonate ions did not initiate any transmission signal during the FTIR investigation of commercial YSZ. The functional groups of the carbonate ions are 1490 cm⁻¹ - 1410 cm⁻¹ (stretching) and 880 cm⁻¹ - 860 cm⁻¹(bending) [20]. For YSC55, YSC64, and YSC73, the broad peak at stretching and acute peak

at the bending vibration were found at wavenumbers between 1430 and 1520 cm^{-1} and 866 cm^{-1} , respectively. Compared to the bending region, the absorption peak at the wavenumber range of 1430–1520 cm^{-1} is wide and intense. As stated by Coates *et al.*, the first absorption during the infrared investigation is often intense and broad. The second absorption, on the other hand, is mild to medium in strength and generates a narrow peak.

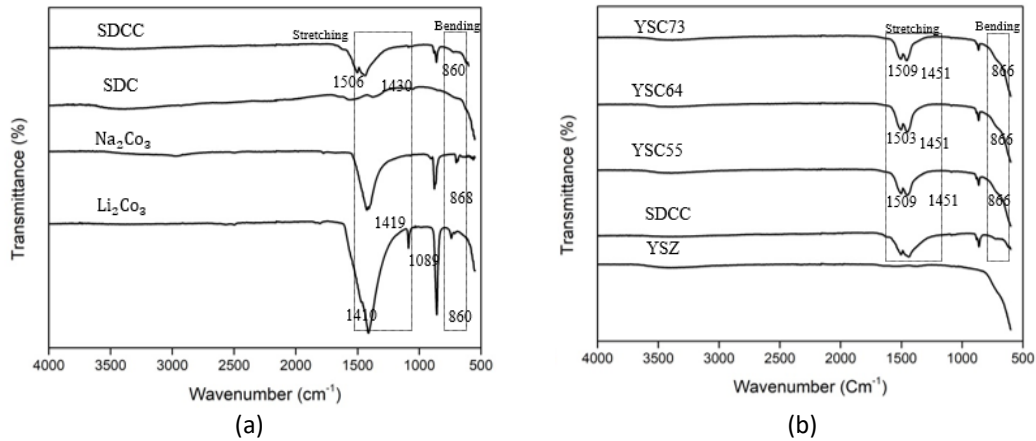


Fig. 6. (a) FTIR spectra of Li_2CO_3 and Na_2CO_3 , SDC and SDCC powders, (b) FTIR spectra for commercial YSZ powder, SDCC composite powder, and YSZ-SDCC composite powders

Figure 7 depicts the FTIR screening of LYSC55, LYSC64, and LYSC73 revealed the CO_3^{2-} bonding transmission signal at 1450, 1451, and 1456 cm^{-1} , respectively. Furthermore, a second transmission signal at 860 cm^{-1} was recorded for each composition. The identified transmission signal is comparable to those found by Ng *et al.*, and Mohammad *et al.*, where the stretching mode start to happened between 1500 cm^{-1} and 1410 cm^{-1} and the bending region occurred between 880 cm^{-1} and 860 cm^{-1} . In specifics, stretching vibration comparison shows that LYSC55 has a sharper peak, followed by LYSC64. The lowest stretching peak can also be seen on the dual composite cathode for LYSC73. This effect happened as a result of decreased absorption in the carbonate transmittance band due to the low composition of the SDCC composite used. As a result of the FTIR investigation, SDCC has strong compatibility with LSCF, YSZ, and SDC materials, as evidenced by the capacity to sustain the presence of carbonate in this YSZ-SDCC composite powders and LSCF/YSZ-SDCC dual composite cathode powders.

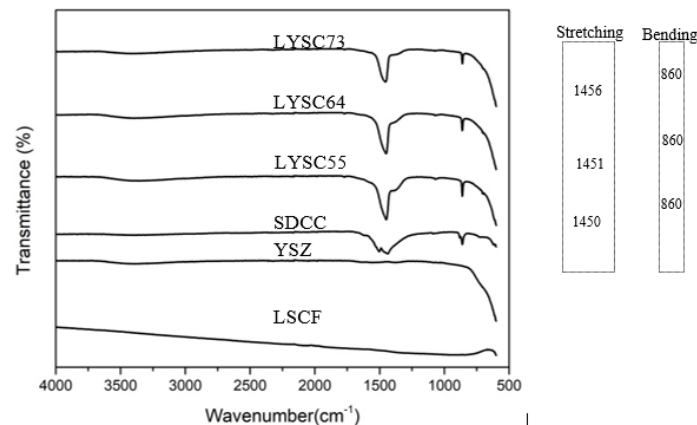


Fig. 7. FTIR spectra for prepared LYSC/YSZ-SDCC dual composite powders

The microstructure of YSZ-SDCC composite cathode powders based on YSZ and SDCC in varying ratios is shown in Figures 8(a-c). Particles of the YSZ-SDCC were seen stacking with one another and the microstructure of the particles exhibits extremely fine structure. The particle size of commercial YSZ and SDC powder before milling and calcining was 379 nm and 130 nm, respectively. Following milling and calcination, all YSZ-SDCC composite cathode powders exhibit consistent particle sizes less than 300 nm. YSC55, YSC64 and YSC73 particles size are 244.97 ± 40.66 nm, 213.47 ± 41.63 nm, and 173.27 ± 25.83 nm. The microstructure of the LSCF/YSZ-SDCC dual composite cathode will not be covered in this study because the findings have previously been reported in a previous publication.

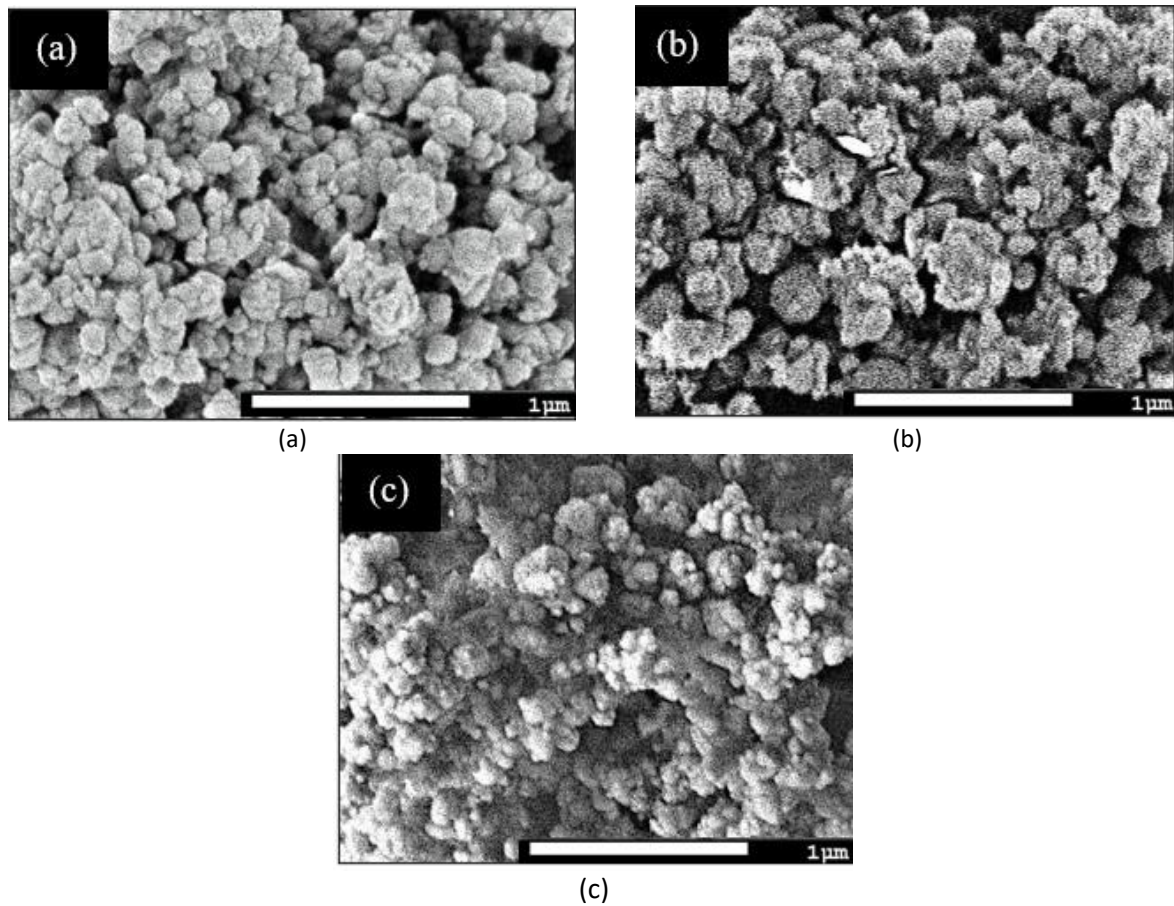


Fig. 8. FESEM micrographs for (a) YSC55, (b) YSC64 and (c) YSC73

3.2 LSCF/YSZ-SDCC Cathode Thin Film Morphology

Figure 9(a-c), show micrographs of the LSCF/YSZ-SDCC cathode thin film screen printed at 10 repetitions, which clearly show non-uniform thickness layer for each composition. The thickness for cathode thin film of LYSC73 is 45.6 ± 1.131 μm, whereas the thickness of LYSC55 is 23.8 ± 0.849 μm, and the thickness of LYSC64 is 32.5 ± 1.626 μm. The average one-time printing results for the LYSC55, LYSC64, and LYSC73 are 2.38 ± 0.085 μm, 3.25 ± 0.163 μm and 4.56 ± 0.113 μm. Simply said, since the mesh size of the screen print is set, the amount of solid content has an impact on the increment and decrement of the screen-printed thickness. Terpeneol formulation is reliant on the quantity of LSCF/YSZ-SDCC ratio applied, thus the calculated amount used in this investigation varied considerably for each composition. The amount of solid content was found to be proportional to the thickness of the cathode layers. Moreover, the measured thicknesses of the dual composite cathode

thin films fell within the 10 μm to 100 μm range, matching a similar finding for printed thin film that was investigated from the previous research [21,22].

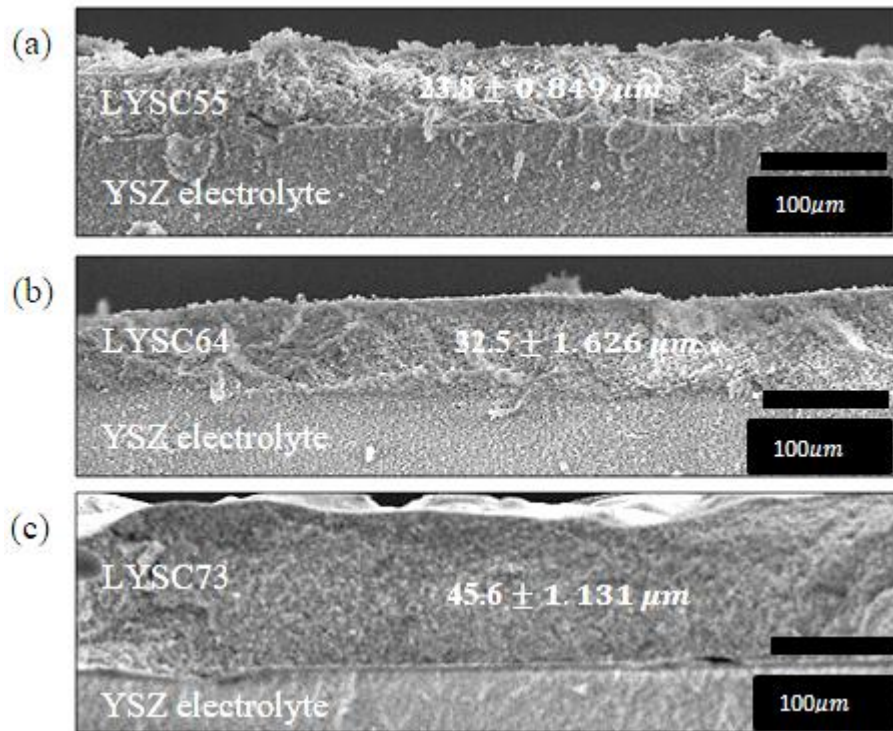


Fig. 9. Micrograph of screen-printed cathode thin film

3.3 Electrochemical Performances of LYSC/YSZ-SDCC

The impedance spectra for the LYSC55, LYSC64 and LYSC73 have been fitted with two equivalent circuit resistances R_{ohm} (R1-CPE1) (R2-CPE2). Resistance and constant phase element were abbreviated as R and CPE. R_{ohm} uses the term to refer to the electrolyte, while R1-CPE1 and R2-CPE2 are the ionic charge transfer and oxygen adsorption/dissociation effects at the cathode-electrolyte interface, respectively [23]. Figure 10 shows the equivalent circuit model that was used to examine the impedance spectrum that was acquired from this investigation.

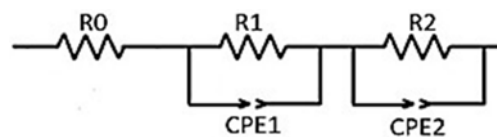


Fig. 10. The equivalent circuit

The Nyquist plot for the LSCF/YSZ-SDCC dual composite cathode is shown in Figure 11(a-c). The sample with the lowest resistance is LYSC55, followed by LYSC64 and LYSC73. This shows that a compound with a higher carbonate composition performs better electrochemical reaction. One semicircle can be observed on the Nyquist plot for the composition parameters studied for LYSC55, LYSC64, and LYSC73. The semicircles on the Nyquist plot represent the interaction between the resistance of the electrolyte within the pores of the cathode components and the resistance of the contact interface between the electrodes and the current collector [24]. The Nyquist plot of LYSC55, LYSC64 and LYSC73 shows that when the operating temperature is lowered, the impedance semicircle curves keep rising, leading to arise in polarization resistance.

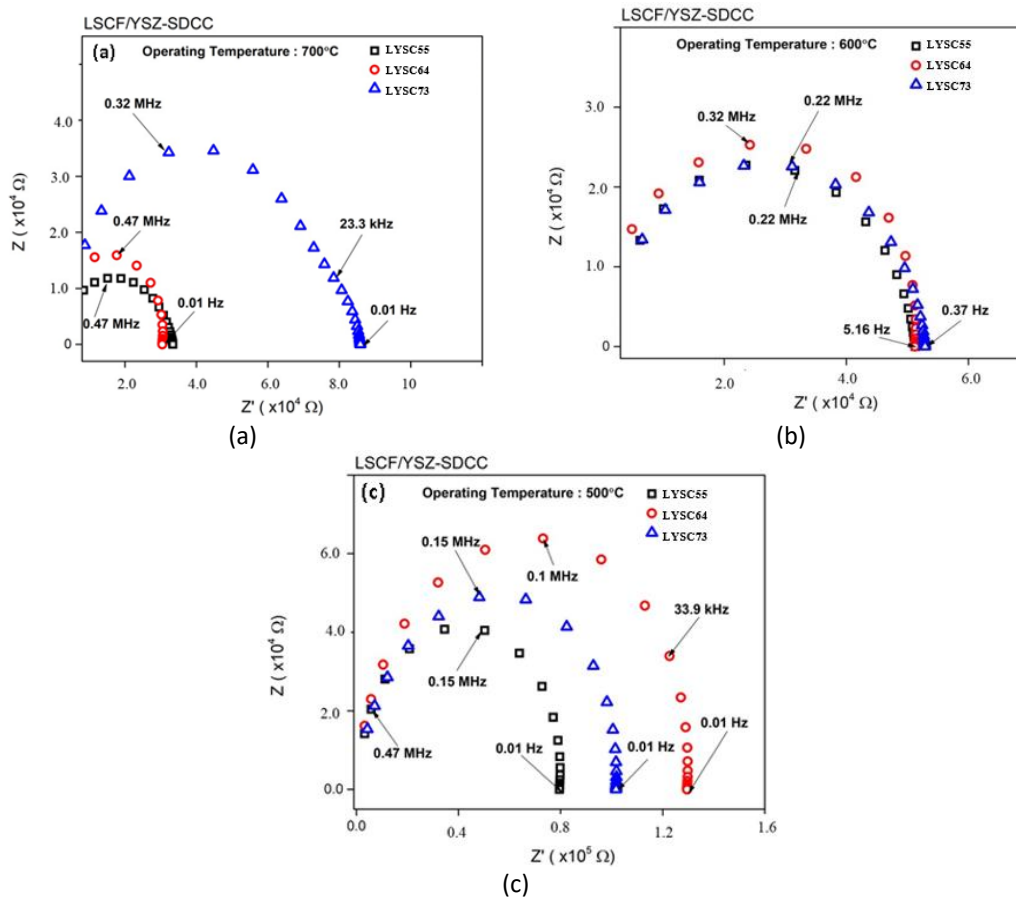


Fig. 11. (a) Nyquist plot at 700°C, (b) Nyquist plot at 600°C and (c) Nyquist plot at 500°C

According to the total resistances listed in Table 2, the total resistances were excessively high, which resulted in the cell's unsatisfactory performance in this study. In comparison to earlier research findings, the calculated ionic conductivity from this study was very low. For standard fuel cell performance at intermediate to low operating temperature, the targeted high ionic conductivity must normally fall within a range of 0.001 - 0.1 Scm^{-1} [25]. Meanwhile, the best ionic conductivity achieved from this investigation was from LYZ 55, with values of $44.232 \times 10^{-6} \text{Scm}^{-1}$. Furthermore, the area specific resistance (ASR) Eq. (2) was used to calculate the electrochemical performance of each dual composite powder. The computed electrochemical performance values for the LYSC55, LYSC64, and LYSC73 sample are presented in Table 3. For this finding, LYSC55 has the minimum ASR values ($1.13 \text{ k}\Omega \text{ cm}^2$) at operating temperature 700°C.

Area specific resistance (ASR) formula:

$$\text{ASR} = (R_p \times S) / 2 \tag{2}$$

where,

R_p : Polarization resistance (Ω)

S: Effective area (cm^2)

Table 2
Electrochemical performances for LYSC55, LYSC64
and LYSC73

Temperatures (°C)	Samples	Conductivity, (σ) [$\times 10^{-6} S cm^{-1}$]	ASR ($k\Omega cm^2$)
700	LYSC55	44.232	1.13
	LYSC64	18.277	2.74
	LYSC73	10.391	4.81
600	LYSC55	21.302	2.35
	LYSC64	10.554	4.98
	LYSC73	9.762	5.12

4. Conclusion

The findings of the phase identification carbonate analysis, morphology, microstructural, and electrochemical performances of prepared powders and cathode thin films were meticulously clarified and validated to finish the final study. In this investigation, LYSC55 were shown to be the most promising composition. Although the ionic conductivity and polarization resistance are outside of the acceptable range, the newly developed dual composite cathode still has a possibility to advance and become highly effective cells at intermediate temperature once all the addressed problems have been resolved. Further suggestions should include optimizing the production of dual composite cathode symmetrical cells. Purity and microstructure of the dual composite cathode should be improved by adjusting the calcination temperature and ensuring that secondary phases are not found. Alternatively, use SDCC or YSZ/SDCC as electrolyte components for the symmetrical cell and perform the TEC test to determine which material is suitable with the LSCF/YSZ-SDCC dual composite cathode. The challenges associated with the development of dual composite cathode materials for intermediate temperatures are more complex. Additional evaluations of physical, chemical, mechanical, and electrochemical properties are required for deeper analysis in the future.

Acknowledgement

The research was supported by the Ministry of Higher Education of Malaysia through funding under the Fundamental Research Grant Scheme (FRGS/1/2020/TK0/UTHM/02/22) and partially funded by Universiti Tun Hussein Onn Malaysia under the Postgraduate Research Grant, REGG (Q205).

References

- [1] Shafie, Shafini Mohd, Zakirah Othman, Norsiah Hami, Salmah Omar, and A. Harits Nu'man. "Solid oxide fuel cells fueled with biogas in Malaysia: A review of potential." *Journal of Advanced Research in Fluid Mechanics and Thermal Sciences* 81, no. 1 (2021): 18-25. <https://doi.org/10.37934/arfmts.81.1.1825>
- [2] Mahato, Neelima, Amitava Banerjee, Alka Gupta, Shobit Omar, and Kantesh Balani. "Progress in material selection for solid oxide fuel cell technology: A review." *Progress in Materials Science* 72 (2015): 141-337. <https://doi.org/10.1016/j.pmatsci.2015.01.001>
- [3] Norman, Nur Wardah, Wan Nor Anasuhah Wan Yusoff, Abdullah Abdul Samat, Mahendra Rao Somalu, Andanastuti Muchtar, and Nurul Akidah Baharuddin. "Fabrication process of cathode materials for solid oxide fuel cells." *Journal of Advanced Research in Fluid Mechanics and Thermal Sciences* 50, no. 2 (2018): 153-160.
- [4] Mahmud, L. S., A. Muchtar, and M. R. Somalu. "Challenges in fabricating planar solid oxide fuel cells: A review." *Renewable and Sustainable Energy Reviews* 72 (2017): 105-116. <https://doi.org/10.1016/j.rser.2017.01.019>
- [5] Rahman, Hamimah Abd, Andanastuti Muchtar, Norhamidi Muhamad, and Huda Abdullah. "Structure and thermal properties of La_{0.6}Sr_{0.4}Co_{0.2}Fe_{0.8}O_{3- δ} SDC carbonate composite cathodes for intermediate-to low-temperature solid oxide fuel cells." *Ceramics International* 38, no. 2 (2012): 1571-1576. <https://doi.org/10.1016/j.ceramint.2011.09.043>

- [6] Abd Aziz, Azreen Junaida, Nurul Akidah Baharuddin, Mahendra Rao Somalu, and Andanastuti Muchtar. "Review of composite cathodes for intermediate-temperature solid oxide fuel cell applications." *Ceramics International* 46, no. 15 (2020): 23314-23325. <https://doi.org/10.1016/j.ceramint.2020.06.176>
- [7] Hermawan, Erik, Gyun Sang Lee, Ghun Sik Kim, Hyung Chul Ham, Jonghee Han, and Sung Pil Yoon. "Densification of an YSZ electrolyte layer prepared by chemical/electrochemical vapor deposition for metal-supported solid oxide fuel cells." *Ceramics International* 43, no. 13 (2017): 10450-10459. <https://doi.org/10.1016/j.ceramint.2017.05.085>
- [8] Tan, Kang Huai, Abd Rahman Hamimah, and Muhammad Izzat Nor. "Addition of Sm_{0.2}Ce_{0.8}O_{1.9} Carbonate into Perovskite Cathode Materials for Low-Temperature Solid Oxide Fuel cell: Short Review." *Journal of Innovation and Technology* 2022, no. 04 (2022): 1-10.
- [9] Tan, K. H., H. A. Rahman, M. S. Azami, U. A. Yusop, N. A. Baharuddin, and MI Nor Ma'arof. "Electrochemical and material characteristics of Ba_{0.5}Sr_{0.5}Co_{0.8}Fe_{0.2}O_{3-δ}Sm_{0.2}Ce_{0.8}O_{1.9} carbonate perovskite cathode composite for low-temperature solid oxide fuel cell." *Ceramics International* 48, no. 23 (2022): 34258-34264. <https://doi.org/10.1016/j.ceramint.2022.07.325>
- [10] Muhammed Ali, S. A., Mustafa Anwar, Nurul Akidah Baharuddin, Mahendra Rao Somalu, and Andanastuti Muchtar. "Enhanced electrochemical performance of LSCF cathode through selection of optimum fabrication parameters." *Journal of Solid State Electrochemistry* 22 (2018): 263-273. <https://doi.org/10.1007/s10008-017-3754-5>
- [11] Hoa, N. K., H. A. Rahman, and M. R. Somalu. "Effects of NiO loading and pre-calcination temperature on NiO-SDCC composite anode powder for low-Temperature solid oxide fuel cells." *Ceramics-Silikaty* 62, no. 1 (2018): 50-58. <https://doi.org/10.13168/cs.2017.0044>
- [12] Baharuddin, Nurul Akidah, Nurul Farhana Abdul Rahman, Hamimah Abd. Rahman, Mahendra Rao Somalu, Mohd Azham Azmi, and Jarot Raharjo. "Fabrication of high-quality electrode films for solid oxide fuel cell by screen printing: A review on important processing parameters." *International Journal of Energy Research* 44, no. 11 (2020): 8296-8313. <https://doi.org/10.1002/er.5518>
- [13] Somalu, Mahendra R., Andanastuti Muchtar, Wan Ramli Wan Daud, and Nigel P. Brandon. "Screen-printing inks for the fabrication of solid oxide fuel cell films: A review." *Renewable and Sustainable Energy Reviews* 75 (2017): 426-439. <https://doi.org/10.1016/j.rser.2016.11.008>
- [14] Bakar, M. S. A., H. A. Rahman, S. F. Mohammad, S. Ahmad, and A. Muchtar. "Morphological and Physical Behaviour of LSCF-SDCC-Ag Composite Cathode with the Incorporation of Ag as an Additive Element." In *Journal of Physics: Conference Series*, vol. 914, no. 1, p. 012011. IOP Publishing, 2017. <https://doi.org/10.1088/1742-6596/914/1/012011>
- [15] Ahmad, S., S. F. Mohammad, H. A. Rahman, H. Taib, A. Ismail, S. M. Salleh, and S. Mahzan. "Comparative Characterization on Structural Properties of Calcined Sm_{0.5}Sr_{0.5}Co_{0.8}O_{3-δ}Sm_{0.2}Ce_{0.8}O_{1.9} Carbonate as Potential Composite Cathode for SOFC." In *IOP Conference Series: Materials Science and Engineering*, vol. 494, no. 1, p. 012003. IOP Publishing, 2019. <https://doi.org/10.1088/1757-899X/494/1/012003>
- [16] Bansal, Narottam P., and Brent Wise. "Sol-gel synthesis of La_{0.6}Sr_{0.4}Co_{0.3-x} and Sm_{0.5}Sr_{0.5}Co_{0.3-x} cathode nanopowders for solid oxide fuel cells." *Ceramics International* 38, no. 7 (2012): 5535-5541. <https://doi.org/10.1016/j.ceramint.2012.03.069>
- [17] Abd Rahman, Hamimah, Linda Agun, Ng Kei Hoa, Sufizar Ahmad, and Nur Azmah Nordin. "Effects of Binary (Lithium/Natrium)(2) Carbonates on the Phase and Microstructural Stability of Lscf-Sdc for Low Temperature Solid Oxide Fuel Cells." *Sains Malaysiana* 49, no. 12 (2020): 3155-3167. <https://doi.org/10.17576/jsm-2020-4912-27>
- [18] Wongmaneerung, R., R. Yimnirun, and S. Ananta. "Effect of two-stage sintering on phase formation, microstructure and dielectric properties of perovskite PMN ceramics derived from a corundum Mg₄Nb₂O₉ precursor." *Materials Chemistry and Physics* 114, no. 2-3 (2009): 569-575. <https://doi.org/10.1016/j.matchemphys.2008.10.003>
- [19] Baharuddin, Nurul Akidah, Andanastuti Muchtar, Mahendra Rao Somalu, and Mohadeseh Seyednezhad. "Influence of mixing time on the purity and physical properties of SrFe_{0.5}Ti_{0.5}O_{3-δ} powders produced by solution combustion." *Powder Technology* 313 (2017): 382-388. <https://doi.org/10.1016/j.powtec.2017.03.035>
- [20] Coates, John. "Interpretation of infrared spectra, a practical approach." (2000). <https://doi.org/10.1002/9780470027318.a5606>
- [21] Zhang, Xiaomin, Li Liu, Zhe Zhao, Baofeng Tu, Dingrong Ou, Daan Cui, Xuming Wei, Xiaobo Chen, and Mojie Cheng. "Enhanced oxygen reduction activity and solid oxide fuel cell performance with a nanoparticles-loaded cathode." *Nano letters* 15, no. 3 (2015): 1703-1709. <https://doi.org/10.1021/nl5043566>
- [22] Piao, Jinhua, Kening Sun, Naiqing Zhang, and Shen Xu. "A study of process parameters of LSM and LSM-YSZ composite cathode films prepared by screen-printing." *Journal of Power Sources* 175, no. 1 (2008): 288-295. <https://doi.org/10.1016/j.jpowsour.2007.09.078>

- [23] Costilla-Aguilar, S. U., M. J. Escudero, R. F. Cienfuegos-Pelaes, and J. A. Aguilar-Martínez. "Double perovskite La₁₋₈Sr_{0.2}CoFeO_{5+δ} as a cathode material for intermediate temperature solid oxide fuel cells." *Journal of Alloys and Compounds* 862 (2021): 158025. <https://doi.org/10.1016/j.jallcom.2020.158025>
- [24] Mei, Bing-Ang, Obaidallah Munteshari, Jonathan Lau, Bruce Dunn, and Laurent Pilon. "Physical interpretations of Nyquist plots for EDLC electrodes and devices." *The Journal of Physical Chemistry C* 122, no. 1 (2018): 194-206. <https://doi.org/10.1021/acs.jpcc.7b10582>
- [25] Zakaria, Zulfirdaus, Saiful Hasmady Abu Hassan, Norazuwana Shaari, Ahmad Zubair Yahaya, and Yap Boon Kar. "A review on recent status and challenges of yttria stabilized zirconia modification to lowering the temperature of solid oxide fuel cells operation." *International Journal of Energy Research* 44, no. 2 (2020): 631-650. <https://doi.org/10.1002/er.4944>